HHS Public Access

Author manuscript

Biomaterials. Author manuscript; available in PMC 2017 July 24.

Published in final edited form as:

Biomaterials. 2016 October ; 105: 156–166. doi:10.1016/j.biomaterials.2016.07.042.

Topical delivery of low-cost protein drug candidates made in chloroplasts for biofilm disruption and uptake by oral epithelial cells

Yuan Liu[1,@], **Aditya C Kamesh**[2,@], **Yuhong Xiao**[2], **Victor Sun**[1], **Michael Hayes**[2], **Henry Daniell**[2,*], and **Hyun Koo**[1,*]

[1]Department of Orthodontics, Divisions of Pediatric Dentistry and Community Oral Health, School of Dental Medicine, University of Pennsylvania, Philadelphia PA 19104-6030

[2]Department of Biochemistry, School of Dental Medicine, University of Pennsylvania, Philadelphia PA 19104-6030

Abstract

Protein drugs (PD) are minimally utilized in dental medicine due to high cost and invasive surgical delivery. There is limited clinical advancement in disrupting virulent oral biofilms, despite their high prevalence in causing dental caries. Poor efficacy of antimicrobials following topical treatments or to penetrate and disrupt formed biofilms is a major challenge. We report an exciting low-cost approach using plant-made antimicrobial peptides (PMAMPs) retrocyclin or protegrin with complex secondary structures (cyclic/hairpin) for topical use to control biofilms. The PMAMPs rapidly killed the pathogen *Streptococcus mutans* and impaired biofilm formation following a single topical application of tooth-mimetic surface. Furthermore, we developed a synergistic approach using PMAMPs combined with matrix-degrading enzymes to facilitate their access into biofilms and kill the embedded bacteria. In addition, we identified a novel role for PMAMPs in delivering drugs to periodontal and gingival cells, 13–48 folds more efficiently than any other tested cell penetrating peptides. Therefore, PDs fused with protegrin expressed in plant cells could potentially play a dual role in delivering therapeutic proteins to gum tissues while killing pathogenic bacteria when delivered as topical oral formulations or in chewing gums. Recent FDA approval of plant-produced PDs augurs well for clinical advancement of this novel concept.

Keywords

Antimicrobial peptide; drug delivery; plant biopharmaceuticals; dental caries; therapeutic enzymes

[*]Co-corresponding authors: Henry Daniell, Ph.D., Professor and Director of Translational Research, School of Dental Medicine, University of Pennsylvania, 240 South 40th St, Rm#547, Levy Building, Philadelphia PA 19104-6030. hdaniell@upenn.edu. Hyun Koo, D.D.S., Ph.D., Professor, Department of Orthodontics, Divisions of Pediatric Dentistry and Community Oral Health School of Dental Medicine, University of Pennsylvania, 240 South 40th St, Rm#417, Levy Building, Philadelphia PA 19104-6030. koohy@upenn.edu.

[@]Both authors made equal contributions

Introduction

Biopharmaceuticals produced in current systems are prohibitively expensive for a large majority of the global population. The cost of protein drugs ($140 billion in 2013) exceeds GDP of >75% of countries around the globe [1], making them unaffordable. One third of global population earns <$2 per day or the low socio-economic/underprivileged in the US can't afford protein drugs. Such high costs are associated with their production in prohibitively expensive fermenters, purification, cold transportation/storage, short shelf life and sterile delivery methods [2,3]. In order to address these concerns, low cost PDs can be made in plant cells for their topical [4] or oral delivery [2,3,5].

Many infectious diseases in humans are caused by biofilms, including those occurring in the mouth [6,7]. For example, dental caries continues to be the single most prevalent biofilm-associated oral disease, afflicting mostly underprivileged children and adults in the US and worldwide, resulting in expenditures of >$40 billion annually [8–10]. Caries-causing (cariogenic) biofilms develop when bacteria interact with dietary sugars and accumulate on tooth surface, forming organized clusters that are firmly adherent and enmeshed in an extracellular matrix of polymeric substances such as exopolysaccharides (EPS) [9]. *Streptococcus mutans* is one of the major pathogens causing dental caries, although additional organisms may be involved [6,8–10]. This bacterium expresses multiple exoenzymes (glucosyltransferases) that make it a primary EPS producer in oral cavity, while it is also highly acidogenic and aciduric [9]. Current topical antimicrobial modalities for controlling cariogenic biofilms are limited. Chlorhexidine (CHX) is considered the 'gold standard' for oral antimicrobial therapy, but has adverse side effects including tooth staining and calculus formation, and is not recommended for daily therapeutic use [11]. As an alternative, several antimicrobial peptides (AMPs) have emerged with potential antibiofilm effects against caries-causing oral pathogens, including *S. mutans* [12,13].

When compared with conventional antibiotics, AMPs provide additional advantages for oral antimicrobial therapy. For example, AMPs not only possess bactericidal activity but also have other biological functions like immunomodulation by activating mast cells and wound healing [14], while playing a critical role in angiogenesis [15]. Furthermore, they are potently active against bacteria (particularly Gram-positive), fungi and viruses and can be tailored to target specific pathogens by fusion with their surface antigens [14,16,17]. AMPs can kill and restrict microbial infection by multiple mechanisms, including altered cell surface charge, disruption of membrane integrity and pore formation while also neutralizing lipopolysaccharides-induced endotoxin shock [14,16–19]. Although development of resistance is less likely with AMPs, previous studies have shown that resistance mechanisms can be developed by pathogens, including up-regulation of proteolytic activity, release of scavenging anionic compounds such as EPS and glycosaminoglycan, as well as amidation and related surface conjugations of membrane lipids and/or peptidoglycan [18,19]. However, AMP structure and bioactivity varies greatly.

Linear AMPs have poor stability or antimicrobial activity when compared to AMPs with complex secondary structures. For example, retrocyclin (RC101) and protegrin-1 (PG1) have

high antimicrobial activity or stability when cyclized [20] or form hairpin structure [21] with formation of disulfide bonds. RC101 is highly stable at pH 3, 4, 7 and temperature 25°C to 37°C as well as in human vaginal fluid for 48 hours [22], while the antimicrobial activity was maintained for up to six months [23]. Likewise, PG1 is highly stable in salt or human fluids [24,25] but potency is lost when linearized. Furthermore, AMPs displaying cyclic or secondary structures have increased penetrability through the microbial membranes compared to linear peptides [26]. These intriguing characteristics of antimicrobial peptides with complex secondary structures may facilitate development of novel therapeutics. However, the high cost of producing sufficient amounts of antimicrobial peptides is a major barrier for their clinical development and commercialization. Therefore, we have produced several low cost antimicrobial peptides (magainin, retrocyclin, protegrin) in plant chloroplasts [14,16,17].

Clinical therapy of biofilm-associated infections faces yet another challenging problem. Antimicrobial drugs often fail to kill the clusters of microbes that are protected by their extracellular matrix in formed biofilms [27–29]. Therefore, EPS-matrix degrading enzymes from fungi (like dextranase or mutanase) have been explored to disrupt biofilm and prevent dental caries [30–33] but with limited success [34,35]. However, a synergistic approach of combining antimicrobial agents with EPS-matrix degrading enzymes has not yet been developed. In order to address the cost of enzymes, we have developed a low cost strategy by producing them in plant chloroplasts [36,37]. Most importantly, plant cells expressing high levels of therapeutic proteins can be lyophilized and stored at room temperature for several years [2,3,38,39].

Apart from treating oral biofilm, protein therapy is minimally utilized in dental medicine because of invasive surgical delivery. However, there is a great need for delivery of growth hormones or other bioactives to enhance cell adhesion, stimulate osteogenesis, bone regeneration, differentiation of osteoblasts or endothelial cells. In addition to minimal patient compliance, injectable protein drugs often do not contain essential information to reach their target cells or cell penetrating capabilities. Therefore, localized targeting and delivery to cells including osteoblasts, periodontal ligament cells, gingival epithelial cells or fibroblasts is essential to advance oral health. When delivered orally, protein drugs synthesized in plant cells can be released by mechanical grinding (chewing). Therefore, in this study, we investigate the specificity or capability of cyclic or acyclic plant-made AMPs (PMAMPs) fused with green fluorescent protein to target various human periodontal or gingival cells and evaluate their efficacy in protein drug delivery. In parallel, we evaluated the potency of PMAMPs to prevent biofilm formation following a topical treatment and their synergistic activities with matrix degrading enzymes for disruption of formed biofilms. Thus, this study reports a new cost-effective approach for production of protein drugs to prevent or treat biofilm-associated oral diseases and deliver PDs to human oral tissues for enhancing oral health.

Materials and Methods

Microorganisms and EPS degrading enzymes

Streptococcus mutans UA159 serotype c (ATCC 700610), *Streptococcus gordonii* DL-1 and *Actinomyces naeslundii* ATCC 12104 were used in present study. The strains tested in this research were selected because *S. mutans* is a well-established virulent cariogenic bacteria [40]. *S. gordonii* is an early colonizer and considered an accessory pathogen (that could enhance virulence of periodontopathogens) [41]. *A. naeslundii* is also detected during the early stages of biofilm formation and may be associated with development of dental root caries [42]. All these strains were grown in ultra-filtered (10 kDa molecular-weight cut-off membrane; Prep/Scale, Millipore, MA) buffered tryptone-yeast extract broth (UFTYE; 2.5% tryptone and 1.5% yeast extract, pH 7.0) with 1% glucose to mid-exponential phase (37°C, 5% CO_2) prior to use. The EPS-degrading enzymes dextranase and mutanase are capable of hydrolyzing α-1,6 glucosidic linkages and α-1,3 glucosidic linkages present in the EPS glucans derived from *S. mutans* [43]. Dextranase produced from *Penicillium* sp. was commercially purchased from Sigma (St. Louis, MO) and mutanase produced from *Trichoderma harzianum* was kindly provided by Dr. William H. Bowen (Center for Oral Biology, University of Rochester Medical Center).

Purification of tag-fused GFP proteins

The transplastomic plants expressing green fluorescence protein (GFP) fused with Cholera Toxin B subunit (CTB), Protein Transduction Domain (PTD), retrocyclin and protegrin were created as described in previous studies [16,38,44,45]. Purification of GFP-fused PG1 or RC101 from transplastomic tobacco was done from 0.2–1 gm of lyophilized plant material. Subsequent downstream processing was done based on protocols established previously [14,16,44] (also see Supplementary Figure S1). The lyophilized material was reconstituted in 10–20 ml of plant extraction buffer (0.2 M Tris HCl pH 8.0, 0.1 M NaCl, 0.01 M EDTA, 0.4 M sucrose, 0.2% Triton X supplemented with 2% phenylmethylsulfonylfluoride (PMSF) and a protease inhibitor cocktail (Pierce). The resuspension was incubated in ice for 1 h with vortex homogenization every 15 min. The homogenates were then sonicated (Misonix sonicator 3000) and spun down at 75,000 g at 4°C for 1 h (Beckman LE-80K optima ultracentrifuge) to obtain the clarified lysate. The lysate was subjected to pretreatment with 70% saturated ammonium sulfate and 1/4th volume of 100% ethanol, followed by vigorous shaking for 2 min. The treated solution was spun down at 2,100 g for 3 min. The upper ethanol phase was collected and the process was repeated with 1/16th volume of 100% ethanol. The pooled ethanol phases were further treated with 1/3rd volume of 5 M NaCl and 1/4th volume of 1-butanol, homogenized vigorously for 2 min and spun down at 2,100 g for 3 min. The lowermost phase was collected and loaded onto a 7 kDa MWCO zeba spin desalting column (Thermo scientific). The desalted extract was injected into a Toyopearl butyl – 650S hydrophobic interaction column (Tosoh bioscience) which was run on a FPLC unit (Pharmacia LKB-FPLC system). The column was equilibrated with 2.3 column volumes of salted buffer (10 mM Tris-HCl, 10 mM EDTA and 50% saturated ammonium sulfate) and unsalted buffer (10 mM Tris-HCl, 10 mM EDTA) to a final 20% salt saturation to facilitate binding of GFP fusions onto the resin. This was followed by a column wash with 5.8 column volumes of salted and unsalted buffer mix and then eluted with unsalted buffer.

The GFP fraction was identified and collected based on the peaks observed in the chromatogram and dialyzed three times in 4°C. The purified proteins were finally lyophilized (labconco freezone 2.5) and then resuspended in sterile 1X PBS for all experiments.

Quantification of purified GFP fusions

Purified GFP-fused RC101 or PG1 were quantified by running on a 12% SDS gel followed by western blot (denatured conditions) or native GFP fluorescence. The western blots were probed using mouse Anti-GFP antibody (Millipore) at 1:3000 dilution followed by secondary probing with 1:4000 dilution of HRP conjugated Goat-Anti Mouse antibody (Southern biotech). GFP fluorescence data was obtained by preparing and running GFP-fusion samples under non-denaturing conditions. The native gels were fluoresced under UV light (Ultraviolet products Inc) and photographed. Commercial GFP standards (Vector labs) were used to quantify GFP fusions by both methods through densitometry using ImageJ software to determine GFP concentration, expression level and yield. Expression level was calculated from GFP concentrations relative to total protein values in plant crude extracts. Yield was determined by multiplying GFP concentration with recovered volume after purification. Individual peptide yield was determined by dividing GFP yield with molar factor 14 (ratio of GFP MW to peptide MW). Total protein was determined by Bradford method.

Evaluation of antibacterial activity of plant-made antimicrobial peptides (PMAMPs)

The antibacterial activity and killing kinetics of PMAMPs (GFP-PG1 and GFP-RC101) against *S. mutans* were analyzed by the determination of minimum inhibitory concentration (MIC) and minimum bactericidal concentration (MBC) as well as time-lapse killing assays as described previously [46]. *S. mutans* were grown to log phase (10^5 CFU/ml), and GFP-PG1 and GFP-RC101 were added to the growth medium at concentrations ranging from 1.25 to 160 μg/ml (two-fold dilution), respectively. At 0, 1, 2, 4, 8 and 24 h, aliquots of bacterial suspensions were serially diluted and plated on agar plates using an automated Eddy Jet spiral plater, and the colony forming units (CFU) colonies were counted. Absorbance at 600 nm was also checked at each time point to measure growth rate. Antibacterial activity against *S. gordonii* and *A. naeslundii* was also determined to compare killing efficacy (vs. *S. mutans*). Time-lapsed confocal fluorescence imaging was also performed to assess the dynamics of *S. mutans* killing at single cell level. GFP-PG1 was added to actively growing (log-phase) *S. mutans* (10^5 CFU/ml) at concentrations of 10 μg/ml in the presence of 2.5 μM propidium iodide-PI (Molecular Probe Inc., Eugene, OR, USA) for labeling dead cells. Confocal images were acquired in the same field of view at 0, 10, 30, and 60 min using Leica SP5-FLIM inverted single photon laser scanning microscope with a 100X (numerical aperture, 1.4) oil immersion objective. The excitation wavelengths were 488 nm and 543 nm for GFP and PI, respectively. The emission filter for GFP was a 495/540 OlyMPFC1 filter, while PI was a 598/628 OlyMPFC2 filter. Images were analyzed by ImageJ 1.44 [47].

In parallel, morphological observations of *S. mutans* treated with PMAMPs (as described above) were also examined by scanning electron microcopy. Actively growing *S. mutans* cells were prepared as described above, and mixed with GFP-PG1 (final concentration of 10

μg/ml) for up to 1 h at 37°C. After treatment, the bacterial cells were collected by filtration (0.4 μm Millipore filter), and then fixed in 2.5% glutaraldehyde and 2.0% paraformaldehyde in 0.1 M cacodylate buffer (pH 7.4) for 1 h at room temperature and processed for SEM (Quanta FEG 250, FEI, Hillsboro, OR) observation. Bacteria treated with buffer only served as control.

Evaluation of anti-biofilm activity of GFP-PG1

S. mutans biofilms were formed on saliva-coated hydroxyapatite (sHA) disc surfaces as detailed previously [47,48]. Hydroxyapatite discs (1.25 cm in diameter, surface area of 2.7 ± 0.2 cm^2, Clarkson, Chromatography Products, Inc., South Williamsport, PA) were coated with filter-sterilized, clarified human whole saliva (sHA) [47]. *S. mutans* was grown in UFTYE medium with 1% (w/v) glucose to mid-exponential phase (37°C, 5% CO_2). Before inoculum, sHA discs were topically treated with GFP-PG1 solution (10 μg/ml) or buffer only (vehicle-control) for 30 min. Chlorhexidine was used as positive control at the same concentration. Then, each of the treated sHA discs were inoculated with 10^5 CFU of actively growing *S. mutans* cells per ml in UFTYE medium containing 1% (w/v) sucrose, and inoculated at 37°C and 5% CO_2 for 19 h. EPS was labeled using 2.5 μM Alexa Fluor 647-labeled dextran conjugate (10 kDa; 647/668 nm; Molecular Probes Inc.), while the bacteria cells were stained with 2.5 μM SYTO9 (485/498 nm; Molecular Probes Inc.). The imaging was performed using multi-photon Leica SP5 confocal microscope with 20X (numerical aperture, 1.00) water immersion objective. The excitation wavelength was 780 nm, and the emission wavelength filter for SYTO 9 was a 495/540 OlyMPFEC1 filter, while the filter for Alexa Fluor 647 was a HQ655/40M-2P filter. The confocal image series were generated by optical sectioning at each selected positions and step size of z-series scanning was 2 μm [47]. Amira 5.4.1 software (Visage Imaging, San Diego, CA, USA) was used to create 3D renderings of biofilm architecture [47,48].

We also examined the effects of PG1, alone or in combination with EPS-degrading enzymes, on pre-formed biofilms. Briefly, *S. mutans* biofilms were allowed to accumulate on untreated sHA discs for 19 h. Then, the biofilms were treated with: 1) vehicle-control, 2) EPS-degrading enzymes only, 3) PG1 only, or 4) PG1 + EPS-degrading enzymes for up to 60 min. A mixture of 100 U dextranase with 20 U mutanase (ratio of 5:1) was used based on optimal enzyme amounts to degrade the EPS-matrix without killing the cells or disturbing the integrity of the biofilm 3D architecture as determined experimental in this study (Supplementary Fig S2) and our previous publication [43]. Alexa Fluor 647-labeled dextran conjugate was used to label the EPS-matrix, while SYTO 9 and PI were used to label live cells and dead cells [47]. Fluorescence images were taken at 0, 10, 30 and 60 min. The biofilm 3D architecture was rendered using AMIRA, and total biomass of EPS, live and dead cells were quantified using COMSTAT and ImageJ. The ratio of live to the total bacteria at each time point was calculated, and the survival rate of live cells (relative to live cells at 0 min) was plotted as described previously [47]. The initial number of viable cells at time point 0 min was considered to be 100%. The percent-survival rate was determined by comparing to time point 0 min [47]. Chlorhexidine at the same concentration was used as a positive control.

To complement the confocal imaging analysis, we also quantified the number of viable cells in each of the biofilms via standard culturing and propidium monoazide (PMA) combined with quantitative PCR (PMA-qPCR) method. At selected time point (19 h), biofilms were removed, homogenized via sonication and subject to microbiological analyses as detailed previously [47–49]; our sonication procedure does not kill bacteria cells while providing optimum dispersal and maximum recoverable counts. Aliquots of biofilm suspensions were serially diluted and plated on blood agar plates using an antomated Eddy Jet Spiral Plater (IUL, SA, Barcelona, Spain). The combination of PMA and qPCR will quantify only cells with intact membrane (i.e. viable cells) because PMA cross-link the DNA of dead cells and extracellular DNA, thereby preventing PCR amplification of DNA from these sources [49]. Briefly, biofilm pellets were resuspended with 500 μl TE (50 mM Tris, 10 mM EDTA, pH 8.0). Using a pipette, the biofilm suspensions were transferred to 1.5 ml microcentrifuge tubes; then mixed with PMA. 1.5 μl PMA (20 mM in 20% dimethyl sulfoxide; Biotium, Hayward, CA) was added to the biofilm suspensions. The tubes were incubated in the dark for 5 min, at room temperature, with occasional mixing. Next, the samples were exposed to light for 3 min (600-W halogen light source). After photo-induced cross-linking, the biofilm suspensions were centrifuged (13,000 g/10 min/4°C) and the supernatant was discarded. The pellet was resuspended with 100 μl TE, following by incubation with 10.9 μl lysozyme (100 mg/ml stock) and 5 μl mutanylysin (5 U/μl stock) (37°C/30 min). Genomic DNA was then isolated using the MasterPure DNA purification kit (Epicenter Technologies, Madison, WI). Ten pictograms of genomic DNA per sample and negative controls (without DNA) were amplified by MyiQ real-time PCR detection system with iQ SYBR Green supermix (Bio-Rad Laboratories Inc., CA) and *S. mutans* specific primer (16S rRNA) as detailed by Klein et al. [49].

Uptake of purified tag-fused GFP proteins and PMAMPs by human oral cell lines

As previously described [44] uptake of GFP fused with CTB, PTD, PG1 and RC101 was studied in human periodontal ligament stem cells (HPDLS), maxilla mesenchymal stem cells (MMS), human head and neck squamous cell carcinoma cells (SCC-1), gingiva-derived mesenchymal stromal cells (GMSC), adult gingival keratinocytes (AGK) and mouse osteoblast cells (OBC). Briefly, 2×10^4 of each cell line were incubated with purified GFP fusion tags in 100 μl PBS/1% FBS at 37°C for 1 h. After fixing with 2% paraformaldehyde and stained with DAPI (Vector laboratories, Inc), all cells were imaged using confocal microscopy. The images were observed under 100X objective, and at least 10–15 GFP-positive cells or images were recorded for each cell line in three independent analysis. Furthermore, the level of fluorescence intensity was determined using ImageJ and at least five area of GFP positive cells were selected to measure the mean GFP density value. The normalized GFP intensity was calculated by dividing the values (mean fluorescence density readings) from GFP fusion proteins by the values from GFP only. To determine the relative GFP fusion tags uptake efficiency by gingiva-derived mesenchymal stromal cells (GMSC) and adult gingival keratinocytes (AGK), GMSC and AGK were cultured in chamber slides at 37°C overnight, followed by incubation with purified GFP fusion proteins at 37°C for 1 h. The level of fluorescence intensity was determined using ImageJ and at least five area of GFP positive cells were selected to measure the mean GFP density value. The normalized

GFP intensity was calculated by dividing the values (mean fluorescence density readings) from GFP fusion proteins by the values from GFP only.

Statistical Analysis

Data are presented as the mean ± standard deviation (SD). All the assays were performed in duplicate in at least two distinct experiments. Pair-wise comparisons were made between test and control using Student's t-test. The chosen level of significance for all statistical tests in present study was $P<0.05$.

Results

Expression and purification of GFP fused antimicrobial peptides from transplastomic plants

Leaves expressing GFP fused antimicrobial peptides RC101 and PG1 (PMAMPs) were harvested from greenhouse and subsequently lyophilized for long-term storage, protein extraction and purification. Expression levels of AMPs were similar to what was reported previously [14,16]. Purification of GFP fused to different antimicrobial peptides (RC101 and PG1) was done in order to test their microbicidal activity against both planktonic and biofilm forming *S. mutans.* Lyophilized leaves expressing different GFP fusions were used for extractions and subsequent downstream processing (Supplementary Fig. S1) to obtain enriched or purified proteins. Quantitation of purified GFP-RC101 and GFP-PG1 by both western blot and native GFP fluorescence gel methods showed high yield of GFP-RC101 (1624 μg of GFP, 116 μg of RC101) per gm of lyophilized leaf (Fig. 1A and 1B). In GFP-PG1 both methods showed lower levels of yield (Fig. 1C and 1D), probably due to unique secondary structures in addition to lower level of expression. The western blots also showed GFP standards at 27 kDa which corresponds to the monomer along with a 54 kDa GFP dimer. In GFP-RC101 western blots, 29 kDa and 58 kDa polypeptides are clearly visible which correspond to the monomer and dimer forms of the fusion (Fig. 1A). This could be attributed to the ability of GFP to form dimers [50]. Native fluorescence of GFP-RC101 and GFP-PG1 (Fig. 1B and 1D) and western blots showed multimeric bands with some of them visible below the 27 kDa GFP standard size which could be because of GFP fusion to cationic peptides causing a electrophoretic mobility shift as described in previous studies [16].

Antibacterial Activity of PMAMPs

We first examined the antimicrobial activity of PMAMPs using dose-response studies. The MIC and MBC values of GFP-PG1 for *S. mutans* were 1.25–2.5 μg/ml and 5–10 μg/ml, while for GFP-RC101 the MIC and MBC were 10–20 μg/ml and 80–160 μg/ml. Furthermore, GFP-PG1 displays potent antibacterial activity (similar to synthetic PG1) against *S. mutans*, a proven biofilm-forming and caries-causing pathogen, rapidly killing the bacterial cells within 1 h at low concentrations (Fig. 2A and 2B). GFP-RC101 was less efficient in killing *S. mutans* than GFP-PG1 at similar concentrations, probably due to impact of GFP fusion on cyclization of retrocyclin (Fig. 2C and 2D). GFP-PG1 also killed other oral bacteria including *S. gordonii* (that could enhance virulence of periodontal pathogens) and *A. naeslundii* (associated with dental root caries) (Fig. 2E). Time-lapse

confocal imaging shows that *S. mutans* viability is affected as early as 10 min as shown in Fig. 3A. SEM imaging revealed disruption of *S. mutans* membrane surface, causing irregular cell morphology as well as extrusion of the intracellular content, while untreated bacteria showed intact and smooth surfaces without any visible cell lysis or debris (Fig. 3B). Having shown potent antimicrobial activity of GFP-PG1 against *S. mutans*, we examined the potential of this PMAMP to prevent biofilm formation or disrupt pre-formed biofilms.

Inhibition of Biofilm Initiation by PMAMP PG1

Preventing the formation of pathogenic oral biofilms is challenging because drugs need to exert therapeutic effects following topical applications. To determine whether GFP-PG1 can disrupt the initiation of biofilm, we treated saliva coated apatitic (sHA) surface (tooth surrogate) with a single topical treatment of GFP-PG1 for 30 min, and then incubated with actively growing *S. mutans* cells in cariogenic (sucrose-rich) conditions. We observed substantial impairment of biofilm formation by *S. mutans* with minimal accumulation of EPS-matrix on the GFP-PG1 treated sHA surface (Fig. 4). The few adherent cell clusters were mostly non-viable compared to control (Supplementary Fig. S3), demonstrating potent effects of GFP-PG1 on biofilm initiation despite topical, short-term exposure. In addition, the inhibition of biofilm formation by PG1 was comparable to equivalent concentration of chlorhexidine (CHX).

Disruption of pre-formed biofilm by PMAMP with or without EPS-degrading enzymes

Cariogenic biofilms already formed on tooth surfaces are notoriously difficult to treat because drugs often fail to reach clusters of pathogenic bacteria (such as *S. mutans*) that are surrounded and enmeshed by an exopolysaccharides (EPS)-rich matrix, protecting them against antimicrobials [9]. EPS-degrading enzymes such as dextranase and mutanase could help digest the matrix of cariogenic biofilms. We first optimized the units of dextranase and/or mutanase required for EPS-matrix disruption (Supplementary Fig. S2), which were devoid of antibacterial effects. As shown in Fig. 5A, the combination of dextranase and mutanase can digest the EPS (in red) and ‘open space’ (see arrows) between the bacterial cell clusters (in green) and ‘uncover’ cells (see arrows). Thus, the combination of PG1 and EPS-degrading enzymes could potentiate the overall antibiofilm effects.

To explore this concept, *S. mutans* biofilms were pre-formed on sHA surface, and treated topically with PG1 and EPS-degrading enzymes (Dex/Mut) either alone or in combination. Time-lapsed confocal imaging and quantitative computational analyses were conducted to analyze EPS-matrix degradation and live/dead bacterial cells within biofilms (Fig. 5B and 5C). The enzymes-peptide combination resulted in more than 60% degradation of the EPS-matrix, while increasing the bacterial killing when compared to either PG1 or Dex/Mut alone. These findings were further validated via standard culturing assays by determining colony forming units. The antibacterial activity of PG1 against *S. mutans* biofilms combined with Dex/Mut was significantly enhanced than either one alone (Fig. 5D). Topical exposure of Dex/Mut alone showed no effects on biofilm cell viability, whereas PG1 alone showed some killing activity (Fig. 5C and 5D). Together, the data demonstrate potential of this combined approach to significantly enhance antimicrobial efficacy of PG1 against

established biofilms. Furthermore, this approach was as effective as chlorhexidine combined with EPS-degrading enzymes (Fig. 5D)

Uptake of GFP fused proteins and PMAMPs by human periodontal and gingival cells

Purified GFP fusion proteins or PMAMPs when incubated with human cultured cells, including human periodontal ligament stem cells (HPDLS), Maxilla mesenchymal stem cells (MMS), head and neck squamous cell carcinoma cells (SCC), gingiva-derived mesenchymal stromal cells (GMSC), adult gingival keratinocytes (AGK) and mouse osteoblast cell (OBC) revealed very interesting results. Although only one representative image of each cell line is presented, uptake studies were performed in triplicate and at least 10–15 images were recorded under confocal microscopy (Fig. 6A–F). Without a fusion tag, GFP did not enter any tested human cell line. Both CTB-GFP and PTD-GFP effectively penetrated all tested cell types, although their localization patterns differed. Upon incubation with CTB-GFP, GFP signals localized primarily to the periphery of HPDLSC and MMSC, with small cytoplasmic puncta in SSC-1, AGK, OBC and large cytoplasmic foci in GMSC. PTD-GFP was observed as small cytoplasmic foci in MMSC, variably sized cytoplasmic puncta in HPDLSC, GMSC, AGK, OBC and both the cytoplasm and the periphery of SCC-1 cells. GFP-PG1 is the most efficient tag in penetrating all tested human cells because GFP uptake in GMSC is 30-fold higher than CTB, 17-fold higher than PTD and 48-fold higher than RC101. Likewise, in AGK cells GFP-PG1 GFP accumulation is 28-fold higher than CTB, 13-fold higher than PTD and 40-fold higher than RC101 (Fig. 6G–H). GFP-PG1 showed exclusively cytoplasmic localization in HPDLSC, SCC-1, GMSC and AGK cells and was localized in both the periphery and cytosol in MMSC, but it is only localized in the periphery of OBC. GFP-RC101 entered SCC-1, GMSC, AGK and OBC, but its localization in HPDLSC was negligible and was undetectable in MMSC cells.

Discussion

Development of new therapies against biofilm-related oral diseases and maintenance of oral health has been limited by enormous economical and drug efficacy hurdles. Therapeutic agents need to be effective following topical applications to either prevent biofilm formation or disrupt formed biofilms. Furthermore, it needs to be affordable and readily accessible for majority of the population affected by oral diseases, especially in lower socio-economic communities [7,8]. Here, we report a novel therapeutic concept for controlling oral biofilms formed by a model cariogenic pathogen and drug delivery to oral cells using chloroplast technology for low-cost production of plant-made antimicrobial peptides (PMAMPs). In cariogenic biofilms, *S. mutans* can rapidly accumulate on tooth surface through EPS production, and help to acidify the local microenvironment promoting the growth of an acidogenic microbiota that eventually leads to the onset of dental caries [6,10,28,51]. Although other acidogenic bacteria contribute to caries pathogenesis, *S. mutans* is a key mediator by assembling an insoluble and diffusion-limiting biofilm EPS matrix [9,51]. Our data reveal that PMAMPs, particularly PG1, can efficiently kill *S. mutans* apparently through bacterial membrane disruption.

The mechanisms of action of PG1 have been explored suggesting bacterial killing by permeabilizing their membranes via pore formation [12]. Indeed, we observed that propidium iodide (PI), a cell-impermeant molecule that only enters cells with damaged membranes, rapidly gain intracellular access following PG1 exposure, while SEM images of PG1 treated bacteria provide further evidence of membrane structure disruption. However, the membrane-destabilizing mechanisms needs further elucidation, which may involve complex surface charge alterations, penetration through lipid bilayer of the membrane and PG1 interactions with negatively charged molecules such as teichoic and lipoteichoic acid [52]. Further studies using ellipsometry, electrochemistry, and neutron reflectometry combined with atomic force microscopy or NMR shall elucidate both the molecular targets and structural changes associated with membrane disruption [53–56]. In addition, the observed selectivity between microbial and mammalian cells is based on the amphipathic nature of antimicrobial peptides (AMPs), a common denominator for AMPs. Mammalian cells contain neutrally charged phosphatidylcholine on the outer cell surface and negatively charged phosphatidyl glycerol in the inner cytoplasmic surface. In contrast, outer surface of bacteria contain negatively charged lipids phosphatidyl serine and phosphatidylglycerol as well as lipopolysaccharides [16, 52]. In gram positive bacteria (lipo)teichoic acids also contribute towards the net negative surface charge hence making bacterial cells more anionic than mammalian cells [16, 52].

Protegrin has been tested in clinical studies to treat oral mucositis in patients receiving chemotherapy in phase II, III clinical studies and lack of toxicity against normal oral cells has been well documented [57,58]. The range of concentrations used in this study (<10 μg/ml) is several-fold less than that used in previous clinical trials and toxicity studies. Furthermore, all human cell lines tested remain morphologically intact after treatment with different GFP-fused peptides as clearly observed in the confocal images, suggesting lack of deleterious cellular effects at the tested concentrations. Plant cells are routinely consumed and therefore impurities in plant cell extracts have no negative impact [59] but this approach significantly reduces the cost by elimination of the expensive purification processes. Plant-made PG1 is highly bioactive with similar efficacy as the synthetic peptide (which cost ~ $650,000/gram [14]), demonstrating low cost potential of PMAMPs for biofilm inhibition. Currently there are no reports of successful production of functional protegrin or retrocyclin in any biological system. They are either chemically synthesized and refolded or expressed as linear or fusion proteins, purified and refolded *in vitro*. Ability to make fully functional PMAMPs facilitates their use in topical oral formulations or in chewing gums, thereby eliminating the purification process and reducing cost.

Although AMPs have demonstrated great potential as antimicrobial agents, there are considerable challenges for their clinical application, including stability of the peptides and their susceptibility to proteolytic degradation. Previous studies have shown that cyclization of linear peptides enhances stability to proteases [60], while PG1 has been also shown to inhibit viral proteases [61]. Furthermore, we found that the presence of saliva (which contains both mammalian and bacterial-derived proteolytic enzymes) did not affect the antibacterial effects of PMAMPs (data not shown), suggesting that the peptides were not degraded and the bioactivity unaffected by the salivary proteases.

The main objective here is to develop a proof of concept that we could use PMAMPs to impair biofilm formation mediated by *S. mutans* using topical treatment akin to clinical situation. Currently, chlorhexidine (CHX) is the most effective antimicrobial agent for topical use despite its adverse effects [6,10,11]. We observed that PG1 was as potent as CHX, causing substantial impairment of biofilm formation with a single topical treatment of a tooth-surrogate surface. Similar to CHX, PG1 is highly cationic which could promote effective binding onto saliva-coated apatitic surfaces, and thereby perform antibacterial activity *in situ*. Several chemically synthesized antimicrobial peptides (AMPs) have been tested against oral bacteria [12], including peptides with enhanced specificity to *S. mutans* [13]. However, their antibiofilm efficacy has been mostly determined using continuous, prolonged exposure to AMPs (several hours) rather than topical exposure and without growing biofilms under cariogenic conditions. Furthermore, synthetic AMPs are mostly linear and expensive to produce while being less stable (vs. cyclic/hairpin), which provide barriers for product development and storage [20–25]. In this study, we show that PMAMPs with complex secondary structure (PG1) is an effective inhibitor of biofilm initiation. However, similar to CHX [47,62,63], PMAMPs alone was less effective against developed *S. mutans* biofilms, which remains one of the major therapeutic challenges.

Cariogenic biofilms are characterized by bacteria forming cluster (microcolonies) that are embedded in EPS matrix, making biofilm treatment and removal extremely difficult [9,28,51,62]. This ultimately promotes microbial adhesion and creates a highly cohesive biofilm that shelters resident organisms from antimicrobials while ensuring firm attachment on tooth surfaces [27–29]. Thus, EPS synthesis makes *S. mutans* a formidable opponent to oral health. Here, we developed a novel synergistic concept of PMAMPs and EPS matrix-degrading enzymes combination to disrupt pre-formed biofilms and kill embedded *S. mutans* cells. The EPS from *S. mutans* are comprised primarily of insoluble (with high content of α1,3 linked glucose) and soluble (mostly α1,6 linked glucose) glucans [9]. Glucanohydrolases, dextranase (α1,6 glucanase) or mutanase (α1,3 glucanase), have been explored to disrupt biofilm and prevent dental caries. However, topical applications of enzymes alone have generated moderate anti-biofilm/anti-caries effects clinically, in part due to lack of antibacterial actions [34,64].

Results presented here show that dextranase and mutanase can effectively digest the EPS covering and surrounding the bacterial clusters, significantly enhancing *S. mutans* killing by PMAMPs (~10-fold increase). The glucanohydrolases alone had minimal effects against bacterial viability supporting previous observations [34,64]. Conversely, PMAMPs exhibit no matrix degrading activity. We infer that matrix structure degradation, especially the α1,3 and α1,6-linked glucan backbone and the branch points 3,4- and 3,6-linked glucose that are optimally digested with mutanase and dextranase [43], facilitated PMAMPs access and killing of the exposed bacterial clusters. However, further studies using time-lapse super-resolution 3D microscopy are required to determine the dynamics of matrix degradation and PMAMPs penetration across the biofilm structure. Because PMAMPs fused with GFP is retaining potent antimicrobial activity, it should facilitate their fusion with EPS digesting enzymes in plant cells for their synergistic activities in degrading the biofilm matrix and killing embedded bacteria. This topical antibiofilm approach based on plant-derived PDs could drastically enhance disruption of virulent biofilms by targeting both the scaffold and

bacterial viability, and advance to the clinic as pioneered by Guy's plant monoclonal antibody for human immunotherapy [4].

Retention of high level antimicrobial activity by protegrin along with GFP fusion opens the door for a number of clinical applications to enhance oral health, beyond disruption of biofilms. Several challenges associated with the high cost and invasive surgical delivery of protein drugs in oral health can be addressed. In addition to biofilm disruption, enhancing wound healing in the gum tissues is an important clinical need. We recently reported that both protegrin and retrocyclin can enter human mast cells and induce degranulation, an important step in the wound healing process [14]. Therefore, antimicrobial peptides protegrin and retrocyclin could play an important role in killing bacteria in biofilms and initiate wound healing through degranulation of mast cells. In addition, it is important to effectively deliver growth hormones or other bioactive proteins to enhance cell adhesion, stimulate osteogenesis, and differentiation of osteoblasts or endothelial cells. Delivery efficacy of GFP fused with each tag, independently, was investigated. CTB is used as an ideal transmucosal carrier for oral drug delivery because it enters all human cell types via GM1 receptors Protein transduction domain (PTDs) are small cationic peptides that function as macromolecular transporters by receptor independent, fluid-phase macropinocytosis (a special type of endocytosis) [59]. Therefore, we used both CTB and PTD fusion tags as positive controls to evaluate the efficiency of antimicrobial peptides penetrating human periodontal and gingival cells. GFP-PG1 is the most efficient tag in entering periodontal or gingival human cells because GFP signal could be detected even at 40–48 fold lower concentrations than GFP-RC101 in GMSC and AGK cells. Indeed, protegrin is more efficient in delivering fusion proteins to human cell lines than any other cell penetrating peptide tested so far. Although there were some variations in intracellular localization, GFP-PG1 effectively entered HPDLSC, SCC-1, GMSC, AGK, MMSC and OBC. In contrast GFP-RC101 entered SCC-1, GMSC, AGK and OBC but its localization in HPDLSC and MMSC cells were poor or undetectable. Therefore, this study has identified a novel role for protegrin in delivering drugs to osteoblasts, periodontal ligament cells, gingival epithelial cells or fibroblasts. It is feasible to release protein drugs synthesized in plant cells by mechanical grinding and protein drugs bioencapsulated in lyophilized plant cells embedded in chewing gums could be an ideal mode of drug delivery for their slow and sustained release for longer duration. This provides an alternative to current oral rinse formulations-short duration of contact of antimicrobials on the gum/dental surface. However, further *in vivo* and clinical studies are required to evaluate the anti-biofilm/anti-caries efficacy as well as targeted, sustained drug-delivery in the oral cavity. Comprehensive *in vivo* studies are underway to demonstrate that PMAMPs can be delivered to gum tissue without cytotoxicity and control biofilm formation/dental caries using appropriate human intra-oral models.

Beyond topical application, protein drugs fused with protegrin expressed in plant cells has the potential to be orally delivered to gum tissues in a non-invasive manner and increase patient compliance. Protein drugs bioencapsulated in plants can be stored for many years at room temperature without losing their efficacy [3,65]. The high cost of current protein drugs is due to their production in prohibitively expensive fermenters, purification, cold transportation/storage, short shelf life and sterile delivery methods. All these challenges could be eliminated using this novel drug delivery concept to prevent biofilm-related

infections and enhance oral health. Recent FDA approval of plant cells for production of protein drugs [1] augurs well for clinical advancement of this novel concept.

Supplementary Material

Refer to Web version on PubMed Central for supplementary material.

Acknowledgments

This study was supported by Bill and Melinda Gates Foundation (OPP1031406), NIH grants R01 HL107904, R01 HL109442 and R01 EY 024564 to Henry Daniell, R01 DE18023 and R01 DE025220 to Hyun Koo. We would like to thank the following for providing cell cultures: Dr. Dana T. Graves (osteoblasts, gingival keratinocytes), Dr. Ahn Lee (gingival mesenchymal, HPLSC, SSC-1), Dr. Sunday Akintoye's (MMS), Dr. Francis Mante (osteoblasts) and Dr. Songtao Shi (periodontal ligament stem cells).

References

1. Walsh G. Biopharmaceutical benchmarks. Nat Biotechnol. 2014; 32:992–1000. [PubMed: 25299917]
2. Kwon KC, Daniell H. Low-cost oral delivery of protein drugs bioencapsulated in plant cells. Plant Biotechnol J. 2015; 13:1017–1022. [PubMed: 26333301]
3. Daniell H, Lin CS, Yu M, Chang WJ. Chloroplast genomes: diversity, evolution and applications in genetic engineering. Genome Biol. 2016; 17doi: 10.1186/s13059-016-1004-2
4. Ma JK, Hikmat BY, Wycoff K, Vine ND, Chargelegue D, Yu L, et al. Characterization of a recombinant plant monoclonal secretory antibody and preventive immunotherapy in humans. Nat Med. 1998; 4:601–606. [PubMed: 9585235]
5. Arntzen C. Plant-made pharmaceuticals: from 'Edible Vaccines' to Ebola therapeutics. Plant Biotechnol J. 2015; 13:1013–1016. [PubMed: 26345276]
6. Flemmig TF, Beikler T. Control of oral biofilms. Periodontol 2000. 2011; 55:9–15. [PubMed: 21134225]
7. Hall-Stoodley L, Costerton JW, Stoodley P. Bacterial biofilms: from the natural environment to infectious diseases. Nat Rev Microbiol. 2004; 2:95–108. [PubMed: 15040259]
8. Kassebaum NJ, Bernabe E, Dahiya M, Bhandari B, Murray CJ, Marcenes W. Global burden of untreated caries: a systematic review and metaregression. J Dent Res. 2015; 94:650–658. [PubMed: 25740856]
9. Bowen WH, Koo H. Biology of Streptococcus mutans-derived glucosyltransferases: role in extracellular matrix formation of cariogenic biofilms. Caries Res. 2011; 45:69–86.
10. Marsh PD, Moter A, Devine DA. Dental plaque biofilms: communities, conflict and control. Periodontol 2000. 2011; 55:16–35. [PubMed: 21134226]
11. Autio-Gold J. The role of chlorhexidine in caries prevention. Oper Dent. 2008; 33:710–716. [PubMed: 19051866]
12. da Silva BR, de Freitas VA, Nascimento-Neto LG, Carneiro VA, Arruda FV, de Aguiar AS, et al. Antimicrobial peptide control of pathogenic microorganisms of the oral cavity: a review of the literature. Peptides. 2012; 36:315–321. [PubMed: 22664320]
13. Guo L, McLean JS, Yang Y, Eckert R, Kaplan CW, Kyme P, et al. Precision-guided antimicrobial peptide as a targeted modulator of human microbial ecology. Proc Natl Acad Sci U S A. 2015; 112:7569–7574. [PubMed: 26034276]
14. Gupta K, Kotian A, Subramanian H, Daniell H, Ali H. Activation of human mast cells by retrocyclin and protegrin highlight their immunomodulatory and antimicrobial properties. Oncotarget. 2015; 6:28573–28587. [PubMed: 26378047]
15. Koczulla R, von Degenfeld G, Kupatt C, Krotz F, Zahler S, Gloe T, et al. An angiogenic role for the human peptide antibiotic LL-37/hCAP-18. J Clin Invest. 2003; 111:1665–1672. [PubMed: 12782669]

16. Lee S, Li B, Jin S, Daniell H. Expression and characterization of antimicrobial peptides Retrocyclin-101 and Protegrin-1 in chloroplasts to control viral and bacterial infections. Plant Biotechnol J. 2011; 9:100–115. [PubMed: 20553419]
17. DeGray G, Rajasekaran K, Smith F, Sanford J, Daniell H. Expression of an antimicrobial peptide via the chloroplast genome to control phytopathogenic bacteria and fungi. Plant Physiol. 2001; 127:852–862. [PubMed: 11706168]
18. Andersson D, Hughes D, Kubicek-Sutherland J. Mechanisms and consequences of bacterial resistance to antimicrobial peptides. Drug Resist Updat. 2016; 26:43–57. [PubMed: 27180309]
19. Nizet V. Antimicrobial peptide resistance mechanisms of human bacterial pathogens. Curr Issues Mol Biol. 2006; 8:11–26. [PubMed: 16450883]
20. Wang W, Cole AM, Hong T, Waring AJ, Lehrer RI. Retrocyclin, an antiretroviral theta-defensin, is a lectin. J Immunol. 2003; 170:4708–4716. [PubMed: 12707350]
21. Chen J, Falla TJ, Liu H, Hurst MA, Fujii CA, Mosca DA, et al. Development of protegrins for the treatment and prevention of oral mucositis: structure-activity relationships of synthetic protegrin analogues. Biopolymers. 2000; 55:88–98. [PubMed: 10931444]
22. Sassi AB, Bunge KE, Hood BL, Conrads TP, Cole AM, Gupta P, et al. Preformulation and stability in biological fluids of the retrocyclin RC-101, a potential anti-HIV topical microbicide. AIDS Res Ther. 2011; 8:27. [PubMed: 21801426]
23. Sassi AB, Cost MR, Cole AL, Cole AM, Patton DL, Gupta P, et al. Formulation development of retrocyclin 1 analog RC-101 as an anti-HIV vaginal microbicide product. Antimicrob Agents Chemother. 2011; 55:2282–2289. [PubMed: 21321138]
24. Lai JR, Huck BR, Weisblum B, Gellman SH. Design of non-cysteine-containing antimicrobial β-hairpins: structure-activity relationship studies with linear protegrin-1 analogues. Biochemistry. 2002; 41:12835–12842. [PubMed: 12379126]
25. Ma Z, Wei D, Yan P, Zhu X, Shan A, Bi Z. Characterization of cell selectivity, physiological stability and endotoxin neutralization capabilities of α-helix-based peptide amphiphiles. Biomaterials. 2015; 52:517–530. [PubMed: 25818457]
26. Mika JT, Moiset G, Cirac AD, Feliu L, Bardají E, Planas M, et al. Structural basis for the enhanced activity of cyclic antimicrobial peptides: the case of BPC194. Biochim Biophys Acta (BBA)-Biomembranes. 2011; 1808:2197–2205. [PubMed: 21586269]
27. Flemming H, Wingender J. The biofilm matrix. Nat Rev Microbiol. 2010; 8:623–633. [PubMed: 20676145]
28. Koo H, Falsetta ML, Klein MI. The exopolysaccharide matrix: a virulence determinant of cariogenic biofilm. J Dent Res. 2013; 92:1065–1073. [PubMed: 24045647]
29. Peterson BW, He Y, Ren Y, Zerdoum A, Libera MR, Sharma PK, et al. Viscoelasticity of biofilms and their recalcitrance to mechanical and chemical challenges. FEMS Microbiol Rev. 2015; 39:234–245. [PubMed: 25725015]
30. Bowen WH. The effect of dextranase on caries activity in monkeys (macaca irus). Caries Res. 1972; 6:75–76.
31. Guggenheim B, Regolati B, Schmid R, Mühlemann H. Effects of the topical application of mutanase on rat caries. Caries Res. 1980; 14:128–135. [PubMed: 6929223]
32. Jiao Y, Wang S, Lv M, Jiao B, Li W, Fang Y, et al. Characterization of a marine-derived dextranase and its application to the prevention of dental caries. J Ind Microbiol Biotechnol. 2014; 41:17–26. [PubMed: 24197466]
33. Otsuka R, Imai S, Murata T, Nomura Y, Okamoto M, Tsumori H, et al. Application of chimeric glucanase comprising mutanase and dextranase for prevention of dental biofilm formation. Microbiol Immunol. 2015; 59:28–36. [PubMed: 25411090]
34. Hull P. Chemical inhibition of plaque. J Clin Periodontol. 1980; 7:431–442. [PubMed: 7012186]
35. Balakrishnan M, Simmonds RS, Tagg JR. Dental caries is a preventable infectious disease. Aust Dent J. 2000; 45:235–245. [PubMed: 11225524]
36. Agrawal P, Verma D, Daniell H. Expression of Trichoderma reesei β-mannanase in tobacco chloroplasts and its utilization in lignocellulosic woody biomass hydrolysis. PloS one. 2011; 6:e29302. [PubMed: 22216240]

37. Jin S, Kanagaraj A, Verma D, Lange T, Daniell H. Release of hormones from conjugates: chloroplast expression of beta-glucosidase results in elevated phytohormone levels associated with significant increase in biomass and protection from aphids or whiteflies conferred by sucrose esters. Plant Physiol. 2011; 155:222–235. [PubMed: 21068365]
38. Kwon KC, Verma D, Singh ND, Herzog R, Daniell H. Oral delivery of human biopharmaceuticals, autoantigens and vaccine antigens bioencapsulated in plant cells. Adv Drug Deliv Rev. 2013; 65:782–799. [PubMed: 23099275]
39. Lakshmi PS, Verma D, Yang X, Lloyd B, Daniell H. Low cost tuberculosis vaccine antigens in capsules: expression in chloroplasts, bio-encapsulation, stability and functional evaluation in vitro. PLoS One. 2013; 8:e54708. [PubMed: 23355891]
40. Ajdic D, McShan WM, McLaughlin RE, Savic G, Chang J, Carson MB, et al. Genome sequence of Streptococcus mutans UA159, a cariogenic dental pathogen. Proc Natl Acad Sci U S A. 2002; 99:14434–14439. [PubMed: 12397186]
41. Whitmore SE, Lamont RJ. The pathogenic persona of community-associated oral streptococci. Mol Microbiol. 2011; 81:305–314. [PubMed: 21635580]
42. Dige I, Raarup MK, Nyengaard JR, Kilian M, Nyvad B. Actinomyces naeslundii in initial dental biofilm formation. Microbiology. 2009; 155:2116–2126. [PubMed: 19406899]
43. Hayacibara MF, Koo H, Smith AMV, Kopec LK, Scott-Anne K, Cury JA, et al. The influence of mutanase and dextranase on the production and structure of glucans synthesized by streptococcal glucosyltransferases. Carbohydr Res. 2004; 339:2127–2137. [PubMed: 15280057]
44. Xiao Y, Kwon KC, Hoffman BE, Kamesh A, Jones NT, Herzog RW, et al. Low cost delivery of proteins bioencapsulated in plant cells to human non-immune or immune modulatory cells. Biomaterials. 2016; 80:68–79. [PubMed: 26706477]
45. Limaye A, Koya V, Samsam M, Daniell H. Receptor-mediated oral delivery of a bioencapsulated green fluorescent protein expressed in transgenic chloroplasts into the mouse circulatory system. FASEB J. 2006; 20:959–961. [PubMed: 16603603]
46. Koo H, Rosalen PL, Cury JA, Park YK, Bowen WH. Effects of compounds found in propolis on Streptococcus mutans growth and on glucosyltransferase activity. Antimicrob Agents Chemother. 2002; 46:1302–1309. [PubMed: 11959560]
47. Xiao J, Klein MI, Falsetta ML, Lu B, Delahunty CM, Yates JR, et al. The exopolysaccharide matrix modulates the interaction between 3D architecture and virulence of a mixed-species oral biofilm. PLoS Pathog. 2012; 8:e1002623. [PubMed: 22496649]
48. Koo H, Xiao J, Klein MI, Jeon JG. Exopolysaccharides produced by Streptococcus mutans glucosyltransferases modulate the establishment of microcolonies within multispecies biofilms. J Bacteriol. 2010; 192:3024–3032. [PubMed: 20233920]
49. Klein MI, Scott-Anne KM, Gregoire S, Rosalen PL, Koo H. Molecular approaches for viable bacterial population and transcriptional analyses in a rodent model of dental caries. Mol oral microbial. 2012; 27:350–361.
50. Ohashi T, Galiacy SD, Briscoe G, Erickson HP. An experimental study of GFP-based FRET, with application to intrinsically unstructured proteins. Protein Sci. 2007; 16:1429–1438. [PubMed: 17586775]
51. Paes Leme AF, Koo H, Bellato CM, Bedi G, Cury JA. The role of sucrose in cariogenic dental biofilm formation--new insight. J Dent Res. 2006; 85:878–887. [PubMed: 16998125]
52. Matsuzaki K. Control of cell selectivity of antimicrobial peptides. Biochim Biophys Acta (BBA)-Biomembranes. 2009; 1788:1687–1692. [PubMed: 18952049]
53. Schmidtchen A, Ringstad L, Kasetty G, Mizuno H, Rutland MW, Malmsten M. Membrane selectivity by W-tagging of antimicrobial peptides. Biochim Biophys Acta (BBA)-Biomembranes. 2011; 1808:1081–1091. [PubMed: 21192916]
54. Ringstad L, Protopapa E, Lindholm-Sethson B, Schmidtchen A, Nelson A, Malmsten M. An electrochemical study into the interaction between complement-derived peptides and DOPC mono-and bilayers. Langmuir. 2008; 24:208–216. [PubMed: 18052298]
55. García-Sáez AJ, Chiantia S, Salgado J, Schwille P. Pore formation by a Bax-derived peptide: effect on the line tension of the membrane probed by AFM. Biophys J. 2007; 93:103–112. [PubMed: 17416629]

56. Fernandez DI, Le Brun AP, Whitwell TC, Sani M, James M, Separovic F. The antimicrobial peptide aurein 1.2 disrupts model membranes via the carpet mechanism. Phy Chem Chem Phy. 2012; 14:15739–15751.
57. Giles FJ, Miller CB, Hurd DD, Wingard JR, Fleming TR, Sonis ST, et al. A phase III, randomized, double-blind, placebo-controlled, multinational trial of iseganan for the prevention of oral mucositis in patients receiving stomatotoxic chemotherapy (PROMPT-CT trial). Leuk Lymphoma. 2003; 44:1165–1172. [PubMed: 12916869]
58. Trotti A, Garden A, Warde P, Symonds P, Langer C, Redman R, et al. A multinational, randomized phase III trial of iseganan HCl oral solution for reducing the severity of oral mucositis in patients receiving radiotherapy for head-and-neck malignancy. Int J Radiat Oncol Biol Phys. 2004; 58:674–681. [PubMed: 14967419]
59. Kwon KC, Daniell H. Oral Delivery of Protein Drugs Bioencapsulated in Plant Cells. Mol Ther. 2016; 5doi: 10.1038/mt.2016.115
60. Rozek A, Powers JS, Friedrich CL, Hancock RE. Structure-based design of an indolicidin peptide analogue with increased protease stability. Biochemistry. 2003; 42:14130–14138. [PubMed: 14640680]
61. Rothan HA, Abdulrahman AY, Sasikumer PG, Othman S, Rahman NA, Yusof R. Protegrin-1 inhibits dengue NS2B-NS3 serine protease and viral replication in MK2 cells. J Biomed Biotechnol. 2012; 2012:251482. [PubMed: 23093838]
62. Hope CK, Wilson M. Analysis of the effects of chlorhexidine on oral biofilm vitality and structure based on viability profiling and an indicator of membrane integrity. Antimicrob Agents Chemother. 2004; 48:1461–1468. [PubMed: 15105093]
63. Van Strydonck DA, Slot DE, Van der Velden U, Van der Weijden F. Effect of a chlorhexidine mouthrinse on plaque, gingival inflammation and staining in gingivitis patients: a systematic review. J Clin Periodontol. 2012; 39:1042–1055. [PubMed: 22957711]
64. Pleszczyńska M, Wiater A, Janczarek M, Szczodrak J. (1→3)-α-d-Glucan hydrolases in dental biofilm prevention and control: A review. Int J Biol Macromol. 2015; 79:761–778. [PubMed: 26047901]
65. Su J, Zhu L, Sherman A, Wang X, Lin S, Kamesh A, et al. Low cost industrial production of coagulation factor IX bioencapsulated in lettuce cells for oral tolerance induction in hemophilia B. Biomaterials. 2015; 70:84–93. [PubMed: 26302233]

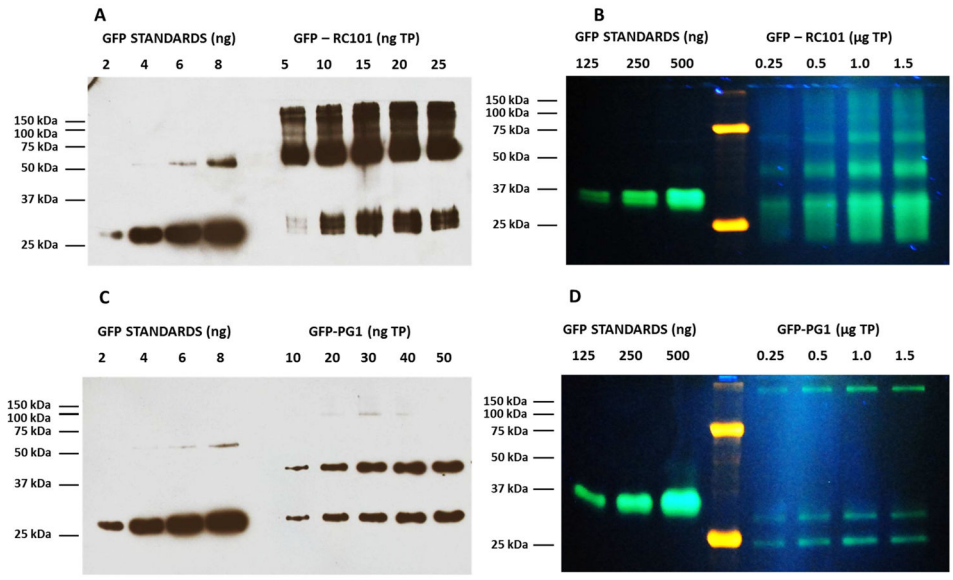

FUSION	AVERAGE EXPRESSION LEVEL (%TP)	PURIFIED GFP YIELD (µg/gm lyophilized material)	PURIFIED PEPTIDE YIELD (µg/gm lyophilized material)	FOLD ENRICHMENT
GFP-RC101	8.80%	1624	116	10.6
GFP-PG1	3.80%	58.8	4.2	4.5

Fig. 1. Purification of GFP-fused Retrocyclin (RC101) and Protegrin (PG1) expressed in tobacco chloroplasts

(A) Western blot analysis of purified GFP-RC101 fusion using Anti-GFP antibody. (B) Native fluorescence gel of purified GFP-RC101 fusion. (C) Western blots of purified GFP-PG1 fusion using Anti-GFP antibody. (D) Native fluorescence gel of purified GFP-PG1.

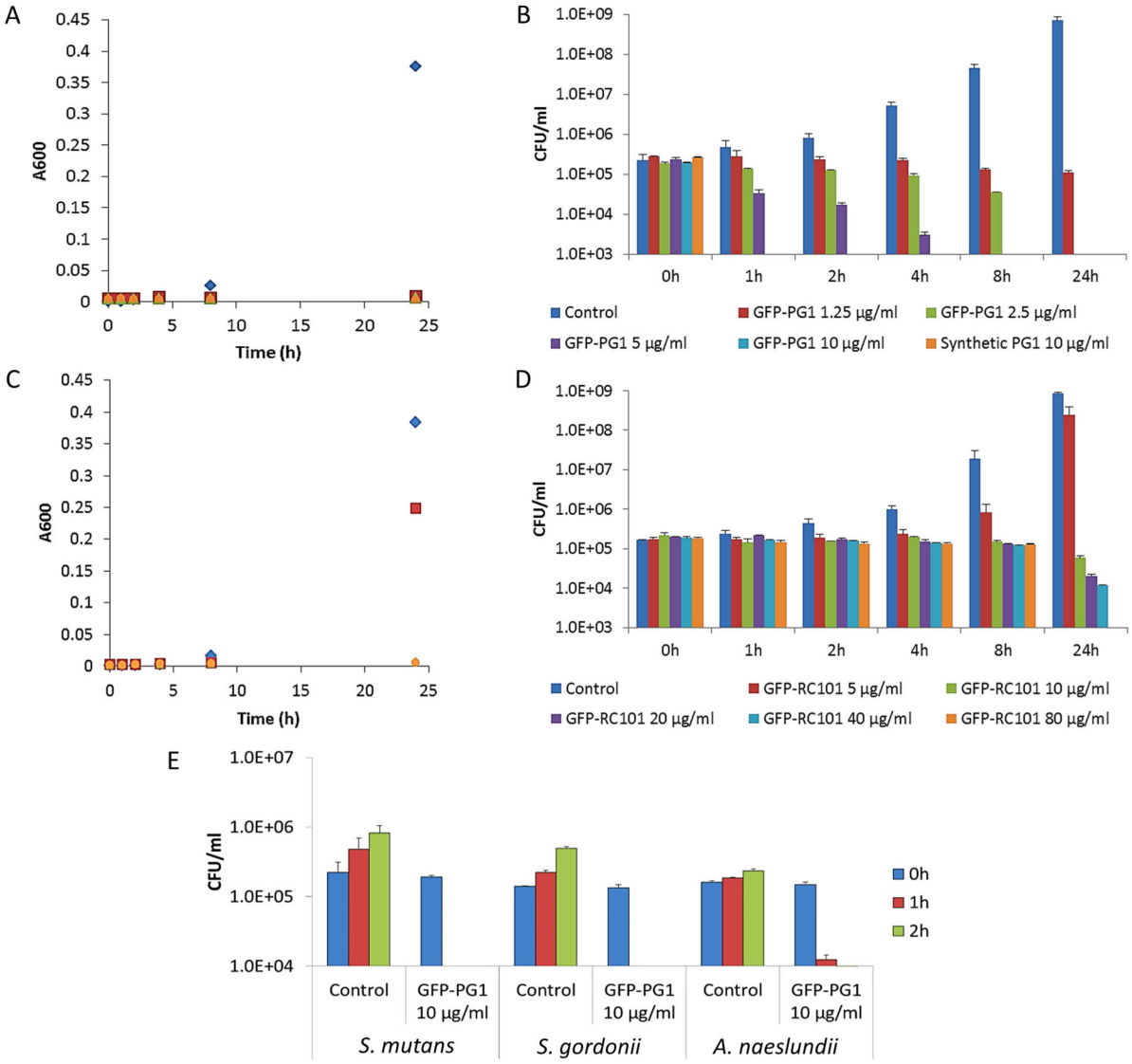

Fig. 2. Antimicrobial activity of PMAMPs (GFP-PG1 and GFP-RC101) against *Streptococcus mutans* and other oral microbes

Cell viability was determined by absorbance (A_{600nm}) and counting colony forming units (CFU) over-time. (A) Time-killing curve of *S. mutans* treated with different concentrations of GFP-PG1 and synthetic PG1 ($A_{600\ nm}$). (B) Viable cells (CFU/ml) of *S. mutans* treated with GFP-PG1 and synthetic PG1 at each time point. (C) Time-killing curve of *S. mutans* treated with GFP-RC101 at different concentrations (A_{600nm}). (D) Viable cells (CFU/ml) of *S. mutans* treated with GFP-RC101 at each time point. (E) Viable cells (CFU/ml) of *S. gordonii* and *A. naeslundii* treated with GFP-PG1 at 10 μg/ml for 1 h and 2 h.

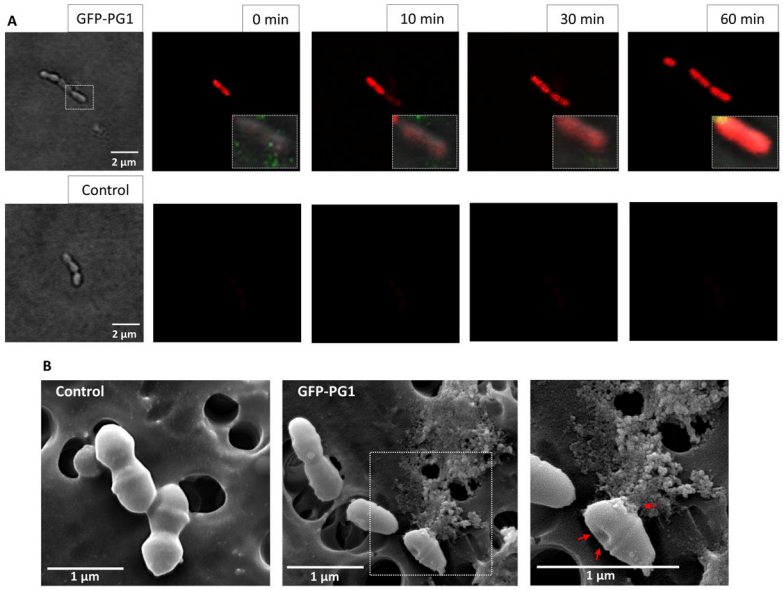

Fig. 3. Bacterial killing by GFP-PG1 as determined via confocal fluorescence (A) and SEM imaging (B)

(A) Time-lapse killing of *S. mutans* treated with GFP-PG1 at 10 μg/ml. The control group consisted of *S. mutans* cells treated with buffer only. Propidium iodide (PI) (in red) was used with confocal microscopy to determine the bacterial viability over time at single-cell level. PI is cell-impermeant and only enters cells with damaged membranes; in dying and dead cells a bright red fluorescence is generated upon binding of PI to DNA. GFP-PG1 is shown in green. (B) Morphological observations of *S. mutans* subjected to GFP-PG1 at a concentration of 10 μg/ml for 1 h using scanning electron microscopy. Red arrows show dimpled membrane and extrusion of intracellular content.

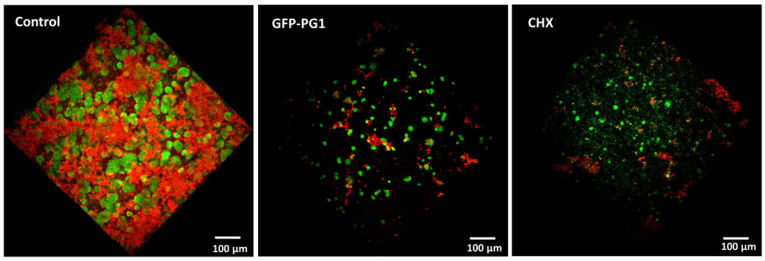

Fig. 4. Inhibition of biofilm formation by a single topical treatment of GFP-PG1

This figure displays representative images of three-dimensional (3D) rendering of *S. mutans* biofilm. Bacterial cells were stained with SYTO 9 (in green) and EPS were labeled with Alexa Fluor 647 (in red). Saliva-coated hydroxyapatite (sHA) disc surface was treated with a single topical treatment of GFP-PG1 or chlorhexidine with a short-term 30 min exposure. The control group was treated with buffer only. Then, the treated sHA disc was transferred to culture medium containing 1% (w/v) sucrose and actively growing *S. mutans* cells (10^5 CFU/ml) and incubated at 37°C, 5% CO_2 for 19 h. After biofilm growth, the biofilms were analyzed by two photon confocal microscopy.

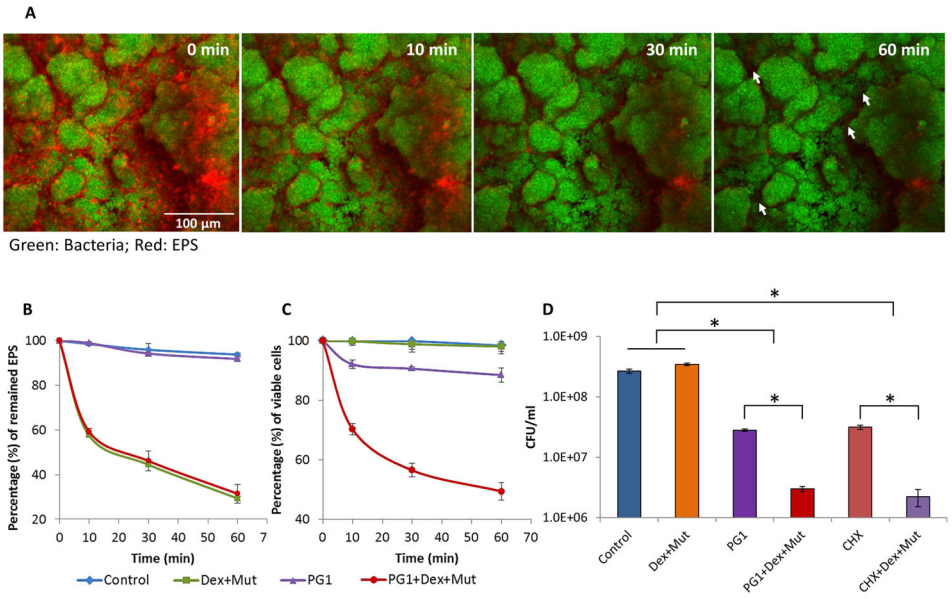

Fig. 5. Biofilm disruption by synthetic PG1 alone or in combination with EPS-degrading enzymes

(A) EPS-degrading enzymes digesting biofilm matrix. Representative time-lapsed images of EPS degradation in *S. mutans* biofilm treated with combination of dextranase and mutanase. Bacterial cells were stained with SYTO 9 (in green) and EPS were labeled with Alexa Fluor 647 (in red). The white arrows show 'opening' of spaces between the bacterial cell clusters and 'uncovering' cells following enzymatic degradation of EPS. (B) Time-lapse quantification of EPS degradation within intact biofilms using COMSTAT. (C) The viability of *S. mutans* biofilm treated with synthetic PG1 and EPS-degrading enzymes (Dex/Mut) either alone or in combination by ImageJ. (D) Antibiofilm activity of synthetic PG1 or chlorhexidine was enhanced by EPS-degrading enzymes (Dex/Mut). Asterisks indicate that the values for different experimental groups are significantly different from each other ($P<0.05$).

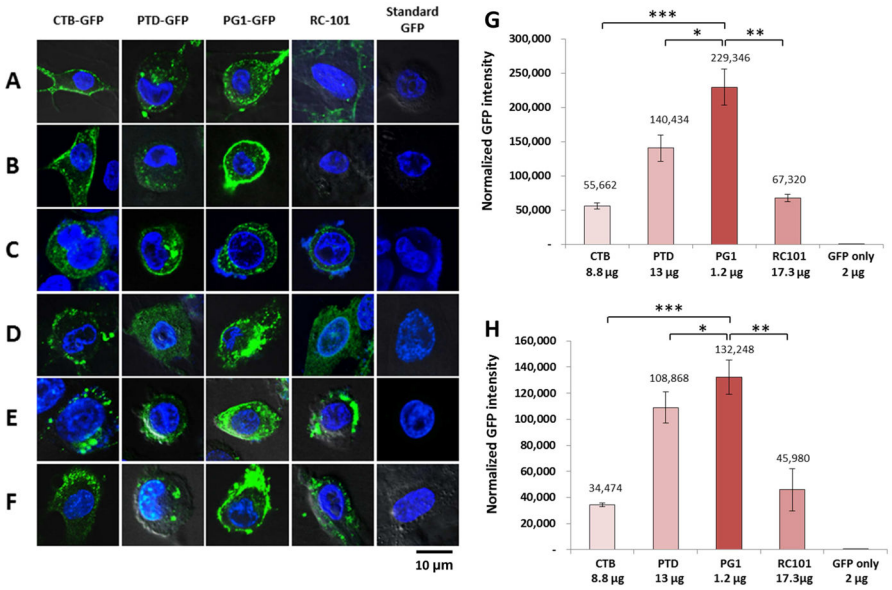

Fig. 6. Uptake of GFP fusion proteins by human periodontal and gingival cells and relative efficiency of GFP fused tags penetrating into human cell lines

(A) Human periodontal ligament stem cells (HPDLS). (B) Maxilla mesenchymal stem cells (MMS). (C) Human head and neck squamous cell carcinoma cells (SCC). (D) Gingiva-derived mesenchymal stromal cells (GMSC). (E) Adult gingival keratinocytes (AGK). (F) Mouse Osteoblast cell (OBC) with confocal microscopy. Human cell lines were cultured as described in the methods section and incubated with GFP or GFP fusion proteins at indicated concentration. Scale bar represent 10 μm. All images studies have been analyzed in triplicate. (G) Gingiva-derived mesenchymal stromal cells (GMSC). (H) Adult gingival keratinocytes (AGK). The GFP intensity were determined using ImageJ. Results are shown as normalized GFP intensity of each GFP fusion protein in cell lines. One-way ANOVA showed significant differences between groups ($P<0.0001$) and *t*-test showed significant differences between two groups (* $P<0.05$, ** $P<0.01$, *** $P<0.001$).